AGU PUBLICATIONS

JGR

Journal of Geophysical Research: Biogeosciences

RESEARCH ARTICLE
10.1002/2014JG002674

Key Points:
- Glacial flour contributed about two thirds of lake diffuse attenuation coefficients
- Turbidity-specific attenuation coefficients increased with glacier distance
- Turbidity-specific attenuation coefficients were similar across regions

Correspondence to:
K. C. Rose,
kev.c.rose@gmail.com

Citation:
Rose, K. C., D. P. Hamilton, C. E. Williamson, C. G. McBride, J. M. Fischer, M. H. Olson, J. E. Saros, M. G. Allan, and N. Cabrol (2014), Light attenuation characteristics of glacially-fed lakes, *J. Geophys. Res. Biogeosci.*, *119*, doi:10.1002/2014JG002674.

Received 21 MAR 2014
Accepted 7 JUL 2014
Accepted article online 10 JUL 2014

Light attenuation characteristics of glacially-fed lakes

Kevin C. Rose[1], David P. Hamilton[2], Craig E. Williamson[3], Chris G. McBride[2], Janet M. Fischer[4], Mark H. Olson[4], Jasmine E. Saros[5], Mathew G. Allan[2], and Nathalie Cabrol[6]

[1]Smithsonian Environmental Research Center, Edgewater, Maryland, USA, [2]Environmental Research Institute, University of Waikato, Hamilton, New Zealand, [3]Department of Biology, Miami University, Oxford, Ohio, USA, [4]Department of Biology, Franklin and Marshall College, Lancaster, Pennsylvania, USA, [5]Climate Change Institute and School of Biology and Ecology, University of Maine, Orono, Maine, USA, [6]The SETI Institute Carl Sagan Center, NASA Ames Research Center, Mountain View, California, USA

Abstract Transparency is a fundamental characteristic of aquatic ecosystems and is highly responsive to changes in climate and land use. The transparency of glacially-fed lakes may be a particularly sensitive sentinel characteristic of these changes. However, little is known about the relative contributions of glacial flour versus other factors affecting light attenuation in these lakes. We sampled 18 glacially-fed lakes in Chile, New Zealand, and the U.S. and Canadian Rocky Mountains to characterize how dissolved absorption, algal biomass (approximated by chlorophyll *a*), water, and glacial flour contributed to attenuation of ultraviolet radiation (UVR) and photosynthetically active radiation (PAR, 400–700 nm). Variation in attenuation across lakes was related to turbidity, which we used as a proxy for the concentration of glacial flour. Turbidity-specific diffuse attenuation coefficients increased with decreasing wavelength and distance from glaciers. Regional differences in turbidity-specific diffuse attenuation coefficients were observed in short UVR wavelengths (305 and 320 nm) but not at longer UVR wavelengths (380 nm) or PAR. Dissolved absorption coefficients, which are closely correlated with diffuse attenuation coefficients in most non-glacially-fed lakes, represented only about one quarter of diffuse attenuation coefficients in study lakes here, whereas glacial flour contributed about two thirds across UVR and PAR. Understanding the optical characteristics of substances that regulate light attenuation in glacially-fed lakes will help elucidate the signals that these systems provide of broader environmental changes and forecast the effects of climate change on these aquatic ecosystems.

1. Introduction

Glaciers are receding globally, with important implications for downstream lakes [*Casassa et al*., 2009; *Hirabayashi et al*., 2010; *Slemmons et al*., 2013]. Early stages of glacial retreat are typically characterized by increased discharge of meltwater, while later stages are characterized by lower water yields due to shrinking upland glaciers [*Casassa et al*., 2009]. Glacial melting may temporarily increase the release of glacial flour, nutrients, and dissolved organic carbon (DOC) to downstream lakes [*Saros et al*., 2010; *Stubbins et al*., 2012]. In turn, these changes may affect the transparency of downstream lakes and the organisms that inhabit them [*Hylander et al*., 2011; *Laspoumaderes et al*., 2013; *Slemmons et al*., 2013]. Complete ablation can amplify the impact of global warming, shifting lakes from cold and turbid to warm and clear [*Vinebrooke et al*., 2010].

Because light affects a number of other critical ecosystem processes [*Williamson and Rose*, 2009, 2010], identification of the material-specific diffuse attenuation coefficients for dissolved substances, phytoplankton, and nonalgal particulates (such as glacial flour) is essential to accurately parameterize lake ecosystem models that link lake physics, chemistry, and biology. Attenuation of incident solar ultraviolet radiation (UVR, ~290–400 nm) and photosynthetically active radiation (PAR, 400–700 nm) regulates numerous physical, chemical, and biological processes and characteristics in aquatic ecosystems, including the depth of the euphotic zone, thermal stratification, and exposure to biologically damaging UVR [*Kirk*, 1994; *Williamson and Rose*, 2009; *Read and Rose*, 2013]. Attenuation of solar radiation is a result of absorption and scattering by a range of substances, including chromophoric dissolved organic matter (CDOM), phytoplankton, and other nonalgal particulates [*Kirk*, 1994]. Changes in climate, land use, and recovery from acidification all have the potential to alter light attenuation, thereby making the attenuation of UVR and PAR sensitive sentinel indicators of environmental change [*Williamson et al*., 2009]. Glacially-fed lake

ecosystems may be particularly sensitive to climate change because they are typically located at high elevations and latitudes where climate change is occurring rapidly [*Immerzeel et al*., 2010]. However, compared to non-glacially-fed lakes, little is known about the variation in processes and optical characteristics of substances regulating UVR and PAR attenuation. Thus, it is difficult to predict the effects of environmental change on glacially-fed lakes.

Variations in DOC and CDOM have been identified as the primary regulators of variation in diffuse attenuation coefficients (K_d) across a wide range of temperate lakes [*Morris et al*., 1995; *Rose et al*., 2009a]. In contrast, glacial particulates (hereafter "glacial flour") can play an important role in regulating attenuation of both UVR and PAR in glacially-fed lakes [*Modenutti et al*., 2000; *Rae et al*., 2001; *Gallegos et al*., 2008]. Thus, while these lakes often have low DOC, they are not necessarily highly transparent [*Sommaruga et al*., 1999]. Further, glacial inputs can cause optical heterogeneity within single systems, with higher light attenuation near glacial inflows [*Modenutti et al*., 2000; *Hylander et al*., 2011]. Currently, the degree to which the quantity and optical qualities of glacial flour vary among sites is unknown due to the lack of comparative studies across multiple glacial regions. Consequently, we are limited in our ability to predict how changes in glacial coverage and discharge affect UVR and PAR attenuation.

In order to develop a predictive understanding of the effects of these substances on UVR and PAR attenuation, we sampled a series of glacially-fed lakes on New Zealand's South Island, the U.S. and Canadian Rocky Mountains, and the Chilean Andes. In this study, we hypothesized that the optical characteristics of attenuating substances in these lakes would be relatively uniform across regions, with glacial flour contributing a majority of the total diffuse attenuation coefficient. This approach highlights the utility of a simple model of diffuse attenuation coefficients and the absorption and scattering estimates used to estimate these coefficients. Our results yield new insights into the relative importance of these substances in regulating light attenuation in glacially-fed lakes and provide a framework for predicting the effects of changing glacial flour inputs on transparency in receiving lakes.

2. Description of Sites

We sampled a total of 18 glacially-fed lakes across several major glaciated regions around the world (Table 1). Seven lakes were on the South Island of New Zealand (Aviemore, Benmore, Ohau, Pukaki, Ruataniwha, Tekapo, and Waitaki), two in the northern United States Rocky Mountains (Grinnell in Glacier National Park, Montana and Rainbow in the Absaroka-Beartooth Wilderness, Montana), two in the Chilean Andes (Lo Encañado and Negra), and seven in the Canadian Rocky Mountains (Amiskwi, Hamilton, Oesa, O'Hara, and Opabin, Vice President, and Secretary Treasurer).

The New Zealand lakes form a lake chain. Ohau, Tekapo, and Pukaki are at the head of this chain and are fed by glaciers in Aoraki/Mount Cook National Park. Outflows from all three lakes have been modified by an extensive hydropower scheme. These three lakes drain into Lake Ruataniwha, a reservoir, before flowing into the Haldon (north) arm of Lake Benmore, another reservoir. The other arm of Benmore, the Ahuriri (west) arm, receives input from its catchment in the National Park and a predominantly pastoral landscape to the southwest. Lake Benmore drains into Lake Aviemore which then drains into Lake Waitaki. The outlet of Lake Waitaki forms the Waitaki River which flows to the Pacific Ocean. All of these lakes are low in DOC, have optical characteristics dominated by glacial flour, and are noted for their turquoise color [*Vant and Davies-Colley*, 1984; *Hamilton et al*., 2004; *Gallegos et al*., 2008] with bedrock composed mostly of granite, greywacke, and metamorphosed schists [*Hamilton et al*., 2013].

The geology of Absaroka-Beartooth Wilderness, USA, is characterized by slow-weathering bedrock dominated by Precambrian granite and crystalline metamorphic rock and contains some of the oldest exposed crust on the North American continent [*Slemmons and Saros*, 2012]. Glacier National Park has an unusual geologic setting as a result of the Lewis Overthrust Fault with carbonate-rich sedimentary rocks over much younger deposits [*Slemmons and Saros*, 2012]. Study sites in the Canadian Rocky Mountains are located in the Bow (O'Hara Oesa and Opabin) and President (Amiskwi, Hamilton, Secretary Treasurer, and Vice President) Ranges. Bow Range bedrock is composed of relatively insoluble quartzite and quartzose sandstone with some carbonate material present in the talus and moraine debris, whereas relatively soluble dolomite limestone dominates the bedrock in the President Range [*Mudry and Anderson*, 1975; *Roy and Hayashi*, 2009].

Table 1. Summary of Glacially-Fed Lake Characteristics[a]

Lake	Latitude	Longitude	Region	Chl *a* ($\mu g\,L^{-1}$)	Turbidity (NTU)	DOC ($mg\,L^{-1}$)	a_{305}	a_{320}	a_{380}	a_{440}	K_d 305	K_d 320	K_d 380	K_d PAR
Amiskwi	51.5924	−116.6440	Canadian Rockies	0.4	2.8	0.3	0.28	0.20	0.09	0.05	0.70	0.58	0.35	0.27
Hamilton	51.4553	−116.5781	Canadian Rockies	0.4	8.4	0.3	0.31	0.23	0.13	0.08	1.40	1.24	1.05	0.60
Oesa	51.3553	−116.3055	Canadian Rockies	0.3	2.2	0.2	0.13	0.10	0.05	0.02	0.49	0.42	0.31	0.21
O'Hara	51.3548	−116.3310	Canadian Rockies	0.5	1.3	0.5	0.57	0.42	0.16	0.07	0.85	0.70	0.33	0.20
Opabin	51.3409	−116.3119	Canadian Rockies	1.9	5.0	0.2	0.41	0.33	0.17	0.09	1.44	1.26	0.91	0.47
Secretary Treasurer	51.5155	−116.5430	Canadian Rockies	0.1	33.5	0.5	0.38	0.29	0.14	0.07	5.78	4.87	3.41	1.35
Vice President	51.5077	−116.5226	Canadian Rockies	0.4	19.8	0.4	0.51	0.40	0.21	0.11	3.91	3.35	2.38	1.07
Lo Encañado	−33.6715	−70.1325	Chile	11.8	8.9	0.4	1.35	1.04	0.39	0.13	4.25	4.39	2.57	0.97
Negra	−33.6572	−70.1219	Chile	0.4	0.3	0.3	0.16	0.10	0.06	0.03	0.26	0.21	0.11	0.09
Aviemore	−44.6211	170.3048	New Zealand	1.3	13.3	NA	0.83	0.65	0.26	0.12	5.84	4.82	2.72	1.16
Benmore[b]	−44.5411	170.1896	New Zealand	1.8	15.0	NA	1.25	0.99	0.39	0.16	6.57	5.59	3.19	1.29
Ohau	−44.2723	169.8703	New Zealand	2.6	24.9	NA	0.47	0.37	0.15	0.08	7.18	6.42	4.38	2.10
Pukaki	−44.1532	170.2168	New Zealand	1.1	45.5	NA	0.16	0.12	0.06	0.04	9.48	7.87	4.94	2.28
Ruataniwha	−44.2797	170.0628	New Zealand	0.9	32.5	NA	0.27	0.21	0.09	0.06	7.70	6.34	3.99	1.97
Tekapo	−43.9955	170.4766	New Zealand	1.2	23.6	NA	0.18	0.14	0.07	0.05	6.05	5.03	3.25	1.54
Waitaki	−44.6764	170.4046	New Zealand	1.5	9.7	NA	0.80	0.63	0.25	0.11	5.10	4.23	2.35	0.96
Grinnell	48.7656	−113.7038	U.S. Rockies	1.0	4.3	0.3	0.86	0.65	0.23	0.08	1.82	1.51	0.89	0.46
Rainbow	45.1337	−109.6961	U.S. Rockies	1.2	1.6	0.7	2.79	2.22	0.83	0.31	3.40	2.67	1.12	0.35

[a]Units of K_d and a_d are in m^{-1}. Latitude and longitude are in decimal degrees. One percent depths can be calculated by dividing 4.605 by K_d.
[b]Benmore values are an average of five sampled sites.

The catchments of Lo Encañado and Negra, Chile, are made up primarily of volcanics (basalt and andesite) covered by the Echaurren glacier above 3500 m. Lahar deposits mark recent to modern interaction between volcanic and glacial activities. Residual frontal moraines on the southern shore of Negra as well as large blocks deposited at the bottom of the lake are granodiorite and residual from the original basin basement that was excavated by glacial erosion.

3. Methods

All lakes were sampled once during summer in 2009, 2010, or 2012. Each lake was sampled in one location with the exception of Benmore which was sampled in five locations. These five samples were averaged to present a single representative observation. Temperature and light attenuation measurements for UVR (305, 320, and 380 nm) and PAR were collected using a Biospherical Instruments Cosine submersible radiometer. Diffuse attenuation coefficients (K_d, unit: m^{-1}) were estimated estimates for each lake's irradiance versus depth relationship, where irradiance at a given depth (E_z) is a function of irradiance at the surface (E_0), the diffuse attenuation coefficient (K_d), and the depth interval (Z) according to the relationship

$$E_z = E_0 e^{-K_d Z} \quad (1)$$

The domains of the regressions were constrained to the log-linear portion of the upper water column, beginning just below the surface and ending before irradiance levels reached detection limits or before a non-log-linear irradiance versus depth relationship was observed. All fits between the ln-linearized irradiance versus depth have a least squares linear regression $R^2 > 0.96$, $p < 0.01$, and the mean R^2 of all regressions was >0.99. Regressions over the upper water column constrained K_d estimates to the depth range above the parent thermocline. Light attenuators such as CDOM, chlorophyll *a*, and turbidity are relatively uniform across

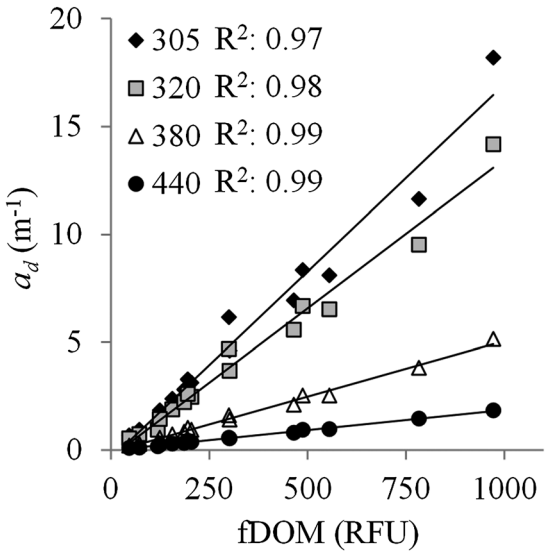

Figure 1. Measurements of fluorescent dissolved organic matter (fDOM) were significantly related to dissolved absorption coefficients (a_d) across 15 lakes, with R^2 values ranging from 0.97 to 0.99 and $p < 0.001$ for all comparisons.

this depth range. It is noted that by constraining estimates to this depth range, processes and characteristics that occur deeper in the water column (such as the presence of a deep chlorophyll maximum) are not considered.

Chlorophyll *a* concentrations were measured in all lakes. In North and South American lakes, chlorophyll *a* was measured in water collected from a depth of 2 m. In New Zealand lakes, only surface samples (0.5 m) were collected. Two samples were collected from each lake. Water was filtered through preashed Whatman GF/F filters, and filters were folded, wrapped in foil, and frozen until analysis immediately upon returning from the field. For North and South American lakes, chlorophyll *a* was extracted using an acetone-methanol mixture, clarified by centrifugation, and corrected for the presence of phaeopigments following the methods of *Pechar* [1987]. In New Zealand lakes chlorophyll *a* was determined fluorometrically after correcting for the presence of phaeopigments using the methods of *Arar and Collins* [1997]. Both methods use a 90% acetone solution, but *Pechar* [1987] includes a brief hot extraction step, and *Arar and Collins* [1997] use a grinding step. Both steps are designed to improve extraction yield. Reported concentrations are the average between the two replicate samples, which differed on average by $< 0.1\ \mu g\ L^{-1}$ (compared with a mean chlorophyll *a* concentration of $1.6\ \mu L^{-1}$). DOC concentrations were measured on water filtered through Whatman GF/F filters using a Shimadzu TOC-V_{CPH} total organic carbon analyzer. DOC was measured in standard sensitivity mode, subtracting Milli-Q deionized water blanks (approximately 0.2 mg C L^{-1}) from standards and samples and calibrating to dilutions of a certified DOC standard (Aqua Solutions, 50 mg L^{-1} potassium biphthalate).

Dissolved absorption coefficients were measured in all lakes. In North and South American lakes, dissolved absorbance was measured with three replicate samples collected from a depth of 2 m. Samples were collected, immediately filtered through Whatman GF/F filters (effective pore size of 0.7 μm), and stored in the cold and dark until analysis. Dissolved absorbance (200–800 nm) was measured using a Shimadzu UV/Visible UV-1650 PC spectrophotometer. Dissolved absorption coefficients (a_{CDOM}, unit: m^{-1}) were calculated at 305, 320, 380, and 440 nm using absorbance measurements (D) and the path length through the quartz cuvette (r) after subtracting Milli-Q water blanks and the average of absorbance at 775–800 nm:

$$a_{CDOM} = (2.303 \times D)/r \quad (2)$$

In New Zealand lakes, dissolved absorption coefficients were estimated from fluorescence dissolved organic matter (fDOM) profiles collected with a Turner Designs C6 fitted with a fDOM sensor, over the depth range where there was a log-linear relationship between PAR irradiance and depth (i.e., the same depth range used to estimate PAR diffuse attenuation coefficients). For example, if we calculated PAR K_d using data from 0.2 to 8 m, then we used the same depth range to calculate turbidity and fDOM. Raw fDOM data were temperature corrected [*Watras et al.*, 2011; *Downing et al.*, 2012]. Next, temperature-corrected data were calibrated to dissolved absorption coefficients using a previously collected in situ calibration data set where fDOM and water for optical scans 200–800 nm were collected simultaneously in 15 lakes (Figure 1). A strong linear relationship was observed between fDOM data and dissolved absorption coefficients; wavelength-dependent coefficients of determination ranged from 0.97 to 0.99 for 305–440 nm. This calibrated relationship between fDOM and dissolved absorption was used to estimate a_{CDOM} for 305, 320, 380, and 440 nm.

Profiles of turbidity were taken in all lakes with a Turner Designs C6 fitted with a nephelometric turbidity sensor. Turbidity measurements were calibrated to a series of standards at 0, 10, and 50 nephelometric turbidity units (NTU). Based on previous studies, turbidity was not high enough to have interfered with the

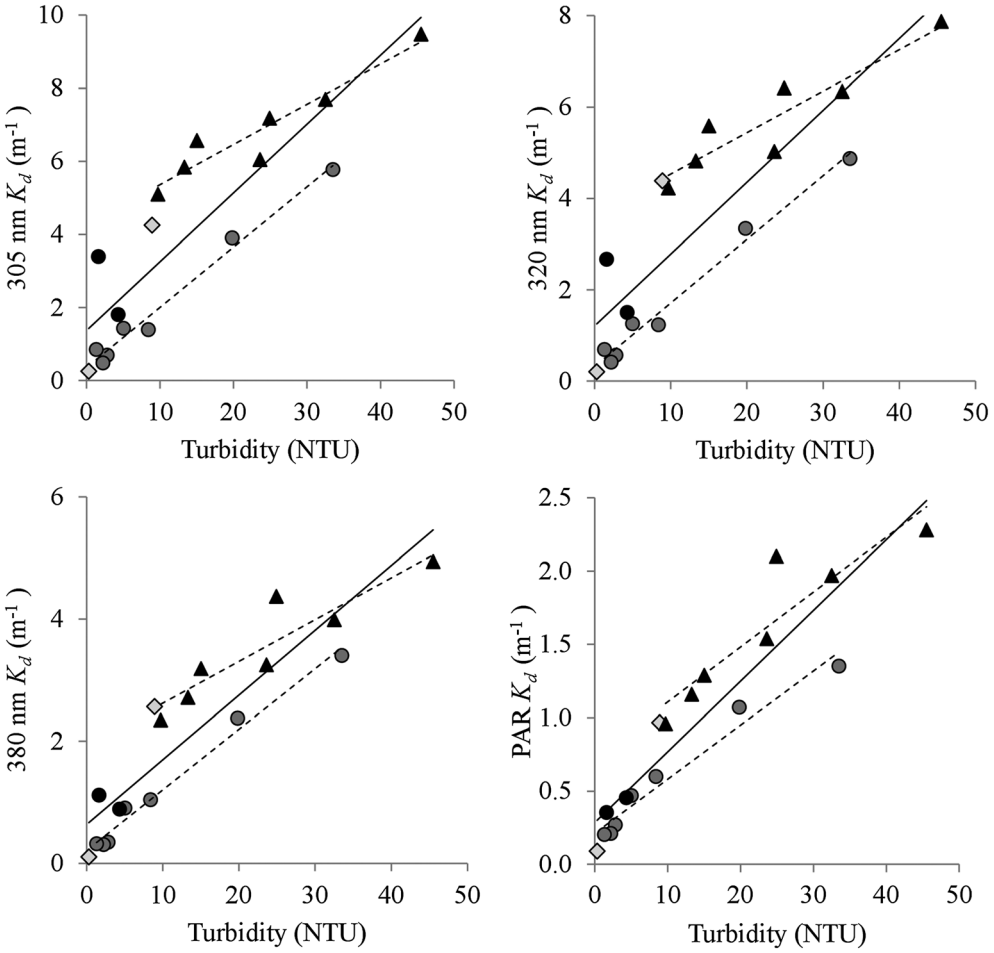

Figure 2. Across all glacially-fed lakes, turbidity, a proxy for glacial flour, was a predictor of K_d (unit: m^{-1}) for UVR wavelengths (305, 320, and 380 nm) and PAR (see Table 2 for statistics). Black triangles represent New Zealand lakes, dark gray circles Canadian Rockies lakes, black circles U.S. Rockies lakes, and light grey diamonds South American lakes. Dashed lines represent regressions for New Zealand lakes or Canadian Rockies lakes and the solid line a regression using all lakes.

fDOM measurements [*Downing et al*., 2012]. Values of turbidity were averaged over the depth range where there was a log-linear relationship between PAR irradiance and depth.

We used an equation of *Kirk* [1994] to partition K_d into multiple constituent attenuation components:

$$K_{d\ \mathrm{total}} = K_{d\ \mathrm{water}} + K_{d\ \mathrm{CDOM}} + K_{d\ \mathrm{algal}} + K_{d\ \mathrm{nap}} \quad (3)$$

where $K_{d\ \mathrm{total}}$ is the total diffuse attenuation coefficient, $K_{d\ \mathrm{water}}$ is diffuse attenuation coefficient due to pure water, $K_{d\ \mathrm{CDOM}}$ is the diffuse attenuation coefficient due to dissolved materials, $K_{d\ \mathrm{algal}}$ is the diffuse attenuation coefficient due to algal particulates, and $K_{d\ \mathrm{nap}}$ is the diffuse attenuation coefficient due to nonalgal particulates. K_d is an apparent optical characteristic, meaning that it is dependent on inherent optical properties and the geometry of the incident light field. Here we estimated component K_d values for UVR and PAR using inherent optical property measurements including the absorption and scattering of different substances and compare these estimates with in situ K_d measurements.

We approximated $K_{d\ \mathrm{water}}$ by using determinations of pure water absorption coefficients (a_w) at the wavelengths of interest, including 305, 320, 380, and 440 nm [*Quickenden and Irvin*, 1980; *Pope and Fry*, 1997]. Dissolved absorption coefficients estimated from either calibration of fDOM measurements or UV/Vis spectrophotometry were used to approximate $K_{d\ \mathrm{CDOM}}$.

We averaged measurements of empirically derived chlorophyll *a*-specific attenuation coefficient estimates from several published studies to estimate $K_{d\ \mathrm{algal}}$ [*Morris et al*., 1995; *Stambler et al*. 1997; *Hodoki and Watanabe*, 1998].

Table 2. Relationships Between Turbidity and K_d Across All Lakes (A, $n = 18$) and Separately Across Lakes in New Zealand (C, $n = 7$) and the Canadian Rockies (E, $n = 7$) and Between Turbidity and the Portion of K_d Not Directly Accounted for by Attenuation Due To Phytoplankton Biomass (as Chlorophyll *a*), Dissolved Absorption or the Absorption of Water ($K_{d\ \text{total}}$–$K_{d\ \text{algal}}$–$K_{d\ \text{CDOM}}$–$K_{d\ \text{water}}$) for All Lakes (B), Lakes in New Zealand (D), and the Canadian Rockies (F)

All Lakes

A	Wavelength	Slope[a]	Intercept	Model Fit (R^2)
	305 nm	0.188	1.371	0.76
	320 nm	0.157	1.210	0.75
	380 nm	0.106	0.648	0.83
	PAR	0.050	0.291	0.84

All Lakes

B	Wavelength	Slope	Intercept	Model Fit (R^2)
	305 nm	0.205	0.183	0.87
	320 nm	0.171	0.261	0.88
	380 nm	0.111	0.231	0.90
	PAR	0.052	0.053	0.86

New Zealand Lakes

C	Wavelength	Slope	Intercept	Model Fit (R^2)
	305 nm	0.110	4.260	0.90
	320 nm	0.091	3.627	0.85
	380 nm	0.068	1.940	0.85
	PAR	0.037	0.735	0.84

New Zealand Lakes

D	Wavelength	Slope	Intercept	Model Fit (R^2)
	305 nm	0.138	2.767	0.99
	320 nm	0.113	2.426	0.97
	380 nm	0.077	1.436	0.91
	PAR	0.041	0.448	0.90

Canadian Rockies Lakes

E	Wavelength	Slope	Intercept	Model Fit (R^2)
	305 nm	0.165	0.364	0.98
	320 nm	0.139	0.320	0.98
	380 nm	0.099	0.213	0.98
	PAR	0.037	0.213	0.96

Canadian Rockies Lakes

F	Wavelength	Slope	Intercept	Model Fit (R^2)
	305 nm	0.165	−0.135	1.00
	320 nm	0.140	−0.069	1.00
	380 nm	0.099	0.028	0.99
	PAR	0.037	0.093	0.98

[a]Slopes (unit: m^{-1} NTU^{-1}) represent estimates of turbidity-specific attenuation coefficients, $p < 0.004$ for all regressions.

Chlorophyll *a*-specific attenuation coefficients used were 0.17 for 305 nm, 0.145 for 320 nm, 0.074 for 380 nm, and 0.07 m^2 (mg Chl *a*)$^{-1}$ for PAR. These empirically derived measurements of chlorophyll *a*-specific attenuation coefficients are higher than laboratory measurements of absorption [*Bricaud et al.*, 1995] because they incorporate both absorption and scattering components. Using these coefficients enabled us to estimate the material-specific diffuse attenuation coefficients from nonalgal particulates to UVR and PAR attenuation by

$$K_{d\,\text{nap}} = K_{d\,\text{total}} - K_{d\,\text{water}} - K_{d\,\text{CDOM}} - K_{d\,\text{algal}} \quad (4)$$

We assumed that attenuation due to nonalgal particulates ($K_{d\ \text{nap}}$) was solely due to glacial flour in glacially-fed lakes. This assumption allowed us to estimate a glacial flour-specific diffuse attenuation coefficient from the slope of the K_d fraction unaccounted for by other attenuating substances versus turbidity. We explore the implications of the assumption that $K_{d\ \text{nap}}$ is exclusively a function of glacial flour in section 5.

Least squares linear regression was used to test relationships between turbidity and diffuse attenuation coefficients. Regressions were considered significant at $p \le 0.05$. Analysis of Covariance (ANCOVA) tests were used to detect differences between turbidity-specific diffuse attenuation coefficients in New Zealand lakes and Canadian Rockies lakes. We also tested if *y* intercepts from regressions between turbidity and diffuse attenuation coefficients were different from zero to evaluate whether other unaccounted for sources of absorption were present in a region. These regions were tested because we sampled a sufficient number of lakes to provide the statistical power necessary to test for differences in estimates of turbidity-specific diffuse attenuation coefficients among regions. To evaluate the relative contributions of DOC, algal biomass, and glacial flour to total diffuse attenuation coefficients, we used estimates of the component attenuation coefficients (from equation (4)) and calculated a proportion of the total attenuation coefficient contributed by each constituent.

4. Results

Across lakes, attenuation of both UVR and PAR was a first-order function of turbidity, a proxy for glacial flour (Figures 2 and 3 and Table 2). Attenuation coefficients were unrelated to chlorophyll *a* (least squares linear regression $p > 0.289$ for all comparisons) or dissolved absorption coefficients (least squares linear regression $p > 0.610$ for all comparisons). The range in observed dissolved absorption coefficients was

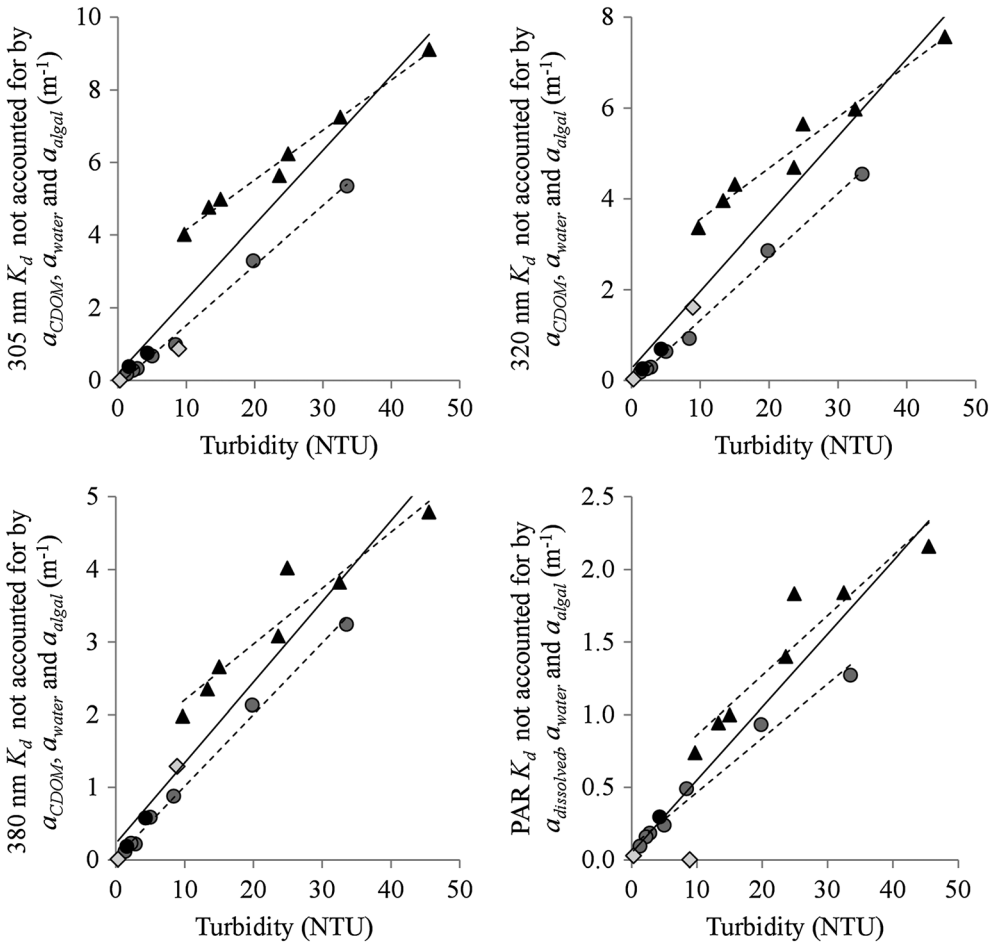

Figure 3. Turbidity was a predictor of the portion of K_d unaccounted for by dissolved substances (a_{CDOM}), algal biomass (a_{algae}), and water (a_{water}) across UVR (305, 320, and 380 nm) and PAR (see Table 2 for statistics). Black triangles represent New Zealand lakes, dark gray circles Canadian Rockies lakes, black circles U.S. Rockies lakes, and light grey diamonds South American lakes. Dashed lines represent regressions for New Zealand lakes or Canadian Rockies lakes and the solid line a regression using all lakes.

relatively narrow and increased with decreasing wavelength (Table 1). The range in K_d values also increased with decreasing wavelength. There was a broad range in turbidity (range: 0.3–45.5 NTU) while chlorophyll *a* was low in all lakes except for Lo Encañado (Table 1; average excluding Lo Encañado: 1.0 μg L^{-1}).

Subtracting estimates of the material-specific diffuse attenuation coefficients for phytoplankton, DOC, and water permitted us to estimate the contributions to attenuation due to turbidity. Overall, the relationships were highly significant (Figure 3 and Table 2; least squares linear regression $p < 0.004$ for all regressions) with turbidity-specific diffuse attenuation coefficients increasing with decreasing wavelength. There was a regional effect on the relationship between turbidity and the portion of K_d not accounted for by a_{CDOM}, a_{algal}, and a_{water} for 305 nm and 320 nm (ANCOVA $p = 0.009$ and 0.027, respectively), indicating that there was a significant difference in turbidity-specific diffuse attenuation coefficients between New Zealand and Canadian Rockies at these wavelengths. However, there was no regional effect at longer wavelengths (380 nm, ANCOVA $p = 0.094$, PAR $p = 0.564$). In New Zealand lakes, *y* intercepts were significantly different from zero across both UVR wavelengths and PAR (*p* range: <0.001–0.039). The *y* intercepts were not different from zero across Canadian Rockies lakes for any UVR wavelength examined (least squares linear regression *p* range: 0.137–0.591) or PAR ($p = 0.057$). *Y* intercepts were not different from zero across all lakes at any wavelengths when lakes were analyzed collectively ($p = 0.197$–0.598).

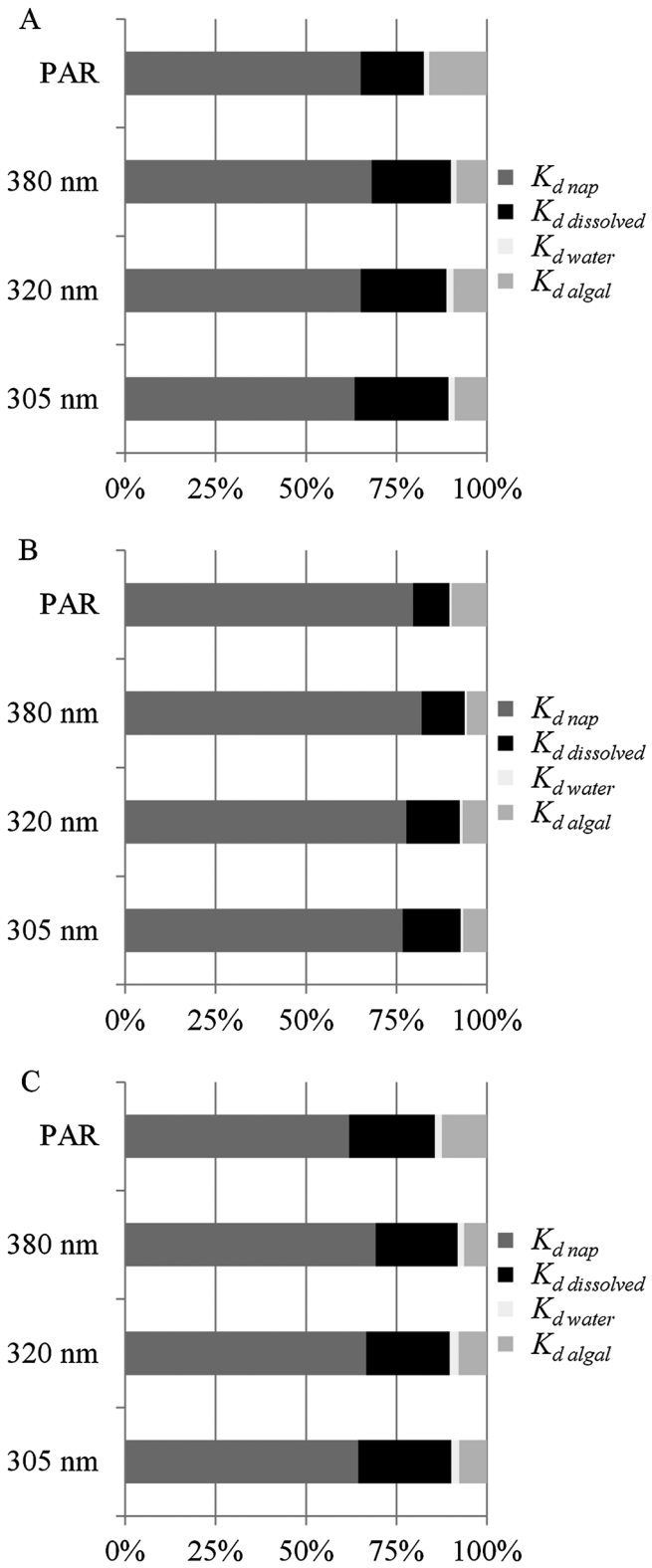

Figure 4. Percentages of the total diffuse attenuation coefficients from nonalgal particulates ($K_{d\ nap}$), dissolved substances ($K_{d\ CDOM}$), water ($K_{d\ water}$), and phytoplankton ($K_{d\ algal}$) with turbidity-specific attenuation coefficients derived in all lakes and applied to all lakes (A), derived from New Zealand lakes and applied to New Zealand lakes (B), and derived from Canadian Rockies lakes and applied to Canadian Rockies lakes (C). Glacial flour is assumed to be the dominant contributor to $K_{d\ nap}$.

Estimating turbidity-specific diffuse attenuation coefficients permitted us to characterize the relative importance of phytoplankton, DOC, water, and glacial flour to total diffuse attenuation coefficients (Figure 4). Across all lakes, glacial flour accounted for approximately two thirds of the total attenuation coefficient for both UVR and PAR (63–68%), while DOC accounted for approximately one quarter of the attenuation for UVR wavelengths and 17% for PAR. Phytoplankton biomass accounted for 8–9% of UVR attenuation and 16% of PAR. Water accounted for only 1–2% of the total K_d across all wavelengths. Using turbidity-specific diffuse attenuation coefficients derived in New Zealand lakes (Table 2D) shows that glacial flour accounted for 77–82% of the total diffuse attenuation across all wavelengths in New Zealand lakes (Figure 4b). Using turbidity-specific diffuse attenuation coefficients derived in Canadian Rocky lakes (Table 2F) shows that glacial flour accounted for 62–69% of the total diffuse attenuation across all wavelengths in Canadian Rocky lakes (Figure 4c).

Along the chain of New Zealand glacially-fed lakes, turbidity-specific diffuse attenuation coefficients increased along the chain of lakes away from those most proximal to glacial inputs (Pukaki, Ohau, and Tekapo; Figure 5). There was a relationship between lake order and turbidity-specific diffuse attenuation coefficients at all measured UVR wavelengths (least squares linear regression 305 nm $R^2 = 0.90$, $p = 0.013$;

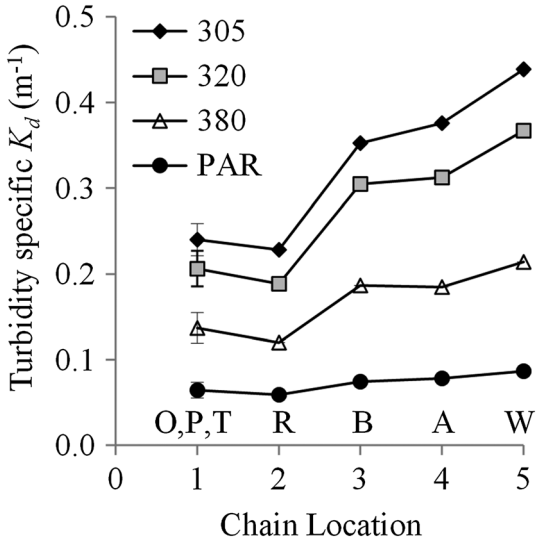

Figure 5. Turbidity-specific K_ds increased with increasing distance (chain location) from glaciers along the chain of New Zealand lakes for UVR (305 nm $R^2 = 0.92$, $p = 0.011$; 320 nm $R^2 = 0.87$, $p = 0.020$; 380 nm $R^2 = 0.81$, $p = 0.036$) but not for PAR ($R^2 = 0.59$, $p = 0.130$). Lakes listed are as follows: Ohau (O), Pukaki (P), Tekapo (T), Ruataniwha (R), Benmore (five-station mean) (B), Aviemore (A), and Waitaki (W). Error bars are standard errors.

320 nm $R^2 = 0.86$, $p = 0.022$; 380 nm $R^2 = 0.80$, $p = 0.041$) and PAR ($R^2 = 0.84$, $p = 0.029$).

5. Discussion

Variation in glacial flour was the primary regulator of variation of both UVR and PAR attenuation in the glacially-fed lakes (Figures 2 and 4). While previous studies have identified glacial flour as an important regulator of light attenuation in isolated glacially-fed systems [*Modenutti et al*., 2000; *Rae et al*., 2001; *Gallegos et al*., 2008], this work is the first to quantify its relative contribution to total diffuse attenuation and to estimate its specific diffuse attenuation coefficients. The results presented here on a broad range of lakes are also the first to compare the optical characteristics of these ecosystems across multiple continents.

We used turbidity as a proxy for glacial flour. Nephelometric turbidity is closely correlated with scattering [*Vant and Davies-Colley*, 1984]. Detailed investigations on the optical characteristics of glacial flour in two of the same South Island lakes sampled in our study show that glacial flour is highly scattering while very weakly absorbing [*Gallegos et al*., 2008]. Additionally, *Rae et al*. [2001] observed attenuation coefficients in glacial Lake Tekapo higher than DOC would alone predict and concluded that this discrepancy was a product of the highly scattering nature of glacial flour. Since the primary mechanism by which glacial flour contributes to attenuation is scattering and not absorption, nephelometric turbidity sensors should provide relatively simple, yet accurate, characterization of glacial flour diffuse attenuation coefficients when other sources of nonalgal particulates are low. However, this type of sensor would not be able to detect whether or not particles vary in absorbance or scattering-to-absorbance ratios, which may induce some error in estimates of glacial flour-specific attenuation coefficients.

The glacial flour-specific diffuse attenuation coefficients estimated here were relatively uniform across lakes and continents, demonstrated by the similar relationships in Figure 3 and the lack of differences between New Zealand and Canadian Rockies turbidity-specific diffuse attenuation coefficients at longer wavelengths. The differences at 305 and 320 nm likely resulted from variation in the size, shape, and source of particulates across catchments and regions. Glacial flour is a product of the underlying local geology in a lake's catchment, and different minerals have distinct size distributions [*Chanudet and Filella*, 2009], which can differentially affect light scattering and absorption [*Kirk*, 1994; *Jonasz and Fournier*, 2007]. Absorption and scattering by inorganic particulates typically increase with decreasing wavelength [*Gallegos et al*., 1990]. Thus, regional differences should be most easily detected at the shortest wavelengths in the ultraviolet range, such as 305 and 320 nm.

We partitioned diffuse attenuation coefficients into multiple components in order to estimate the relative contributions of DOC, phytoplankton, water, and glacial flour to light attenuation. In estimating the diffuse attenuation coefficient due to these constituent substances, we made several simplifications. For example, we assumed that $K_{d\ \mathrm{water}}$ was approximated by $a_{d\ \mathrm{water}}$ and that $K_{d\ \mathrm{CDOM}}$ was approximated by a_{CDOM}. The reality is that the attenuation of incoming solar radiation is an apparent optical property dependent on the geometry of the light field and the inherent optical properties of scattering and absorption. Scattering can increase the path length of incoming solar radiation, which can increase the probability of absorption by dissolved or particulate matter [*Kirk*, 1994]. Thus, $K_{d\ \mathrm{CDOM}}$ is slightly higher than approximated by a_{CDOM}. This difference between is likely to be small in our study lakes for several reasons. First, these glacially-fed lakes had very low concentrations of dissolved and organic

particulate absorbing substances such as DOC and phytoplankton. Therefore, interactions between forward scattering, which changes the forward direction of light underwater, and absorbance were likely minor relative to backscattering, where light is scattered back toward the surface. Additionally, more complex optical models show that the effect of forward scattering has only a minor effect on diffuse attenuation coefficients relative to backscattering loss of light [*Lee et al*., 2005]. Variation in algal biomass and error associated with K_d algal could have contributed to some discrepancy between measured and modeled K_d values. In Figure 3, the lake with the largest residual for PAR was Lo Encañado, which also had the highest chlorophyll *a* concentration (11.8 $\mu g\, L^{-1}$). This might be due to the fact that algae can vary in their absorption characteristics and chlorophyll *a* to algal biomass ratios can vary. Some algae also produce UV-absorbing compounds which can affect K_d estimates [*Laurion et al*., 2000]. Additionally, many high-elevation lakes form a deep chlorophyll maximum (DCM) [*Saros et al*., 2005]. While we estimated light attenuation coefficients in the upper water column, the presence of a DCM would increase the relative importance of K_d algal deeper in the water column. If unaccounted for processes and substances were important in regulating light attenuation, we would expect that the intercepts would be significantly different than zero in our models (Figure 3). Across all lakes and for each wavelength, intercepts were not different than zero (p ranged 0.197–0.598 for all wavelengths). However, when lakes were assessed regionally, intercepts were different from zero for all wavelengths across New Zealand lakes (range of $p < 0.001$–0.039). This suggests that unaccounted for processes, such as nonalgal particulate absorption, were important at these wavelengths in the New Zealand lakes.

We observed an increase in the turbidity-specific light attenuation coefficients along the chain of New Zealand lakes (Figure 5). This increase may be explained if our assumption that glacial flour was the sole contributor to $K_{d\ nap}$ was incorrect, especially in lakes lower in this New Zealand chain. The fact that the *y* intercepts were significantly different from zero for New Zealand lakes in Figure 3 suggests that unmodeled characteristics contribute to attenuation in these lakes. Our model did not incorporate scattering by phytoplankton or absorption by nonalgal particulates. Chlorophyll *a*, an indicator of algal biomass, did not change along this lake chain ($p = 0.922$), implying that changes in algal scattering to total attenuation were probably not the driver of this increase in turbidity-specific attenuation coefficients. Rather, the increase in turbidity-specific attenuation may be due to a gradual change in the source of particulates away from upstream glaciers, to sources with higher relative organic content in lakes further along the chain. Lake Benmore had two major inputs. The Ahuriri arm of Lake Benmore receives input from both the glaciated Aoraki/Mount Cook National Park and the surrounding pastoral landscape, meaning that inputs there may be more organic in nature. Organic particles tend to have higher absorption to scattering ratios compared with inorganic glacial flour [*Gallegos et al*., 2008]. This could explain the high *y* intercept and increasing turbidity-specific absorption along this lake chain. Along this chain of lakes, the ratio of diffuse attenuation coefficients at 320 nm relative to PAR (320 nm UV K_d: PAR K_d) increased. Other studies have shown that an increase in this K_d ratio is consistent with increasingly terrestrial organic inputs [*Rose et al*., 2009b]. Additionally, sorption of DOC to inorganic particulates may also occur as inorganic particles move along this lake chain, which would also increase the absorption to scattering ratio of particles [*Binding et al*., 2008]. Changes in phytoplankton chl:biomass ratios or particle size as a result of light and nutrient regimes, or differential settling, or differential zooplankton grazing may also play some role in the changes along this lake chain.

The substances regulating light attenuation in glacially-fed lakes are very different than most non-glacially-fed lakes. Among the lakes we sampled, glacial flour contributed on average about two thirds of the total attenuation coefficient, while dissolved absorption coefficients contributed only about one quarter to UVR and 17% of PAR (Figure 4). This is in contrast with non-glacially-fed lakes, where dissolved absorbance is typically highly correlated with diffuse attenuation coefficients, especially at short wavelengths [*Morris et al*., 1995; *Markager and Vincent*, 2000; *Rose et al*., 2009a]. Because glacial flour accounted for about two thirds of diffuse attenuation coefficients across these glacially-fed lakes, changes in glacial discharge and flour are likely to have important implications for the transparency of these and other glacially-fed systems. For example, in extreme cases where glaciers completely ablate and glacial water inputs are reduced to zero, the portion of the total diffuse attenuation coefficient that is attributable to glacial flour could also be reduced to zero. In this example, the penetration depth of UVR and PAR would triple. However, it should be noted that over the longer term, glacial retreat and increasing vegetation should increase terrestrial organic matter inputs which would likely reduce K_d values, especially at shorter wavelengths where DOC absorbs more

strongly [*Rose et al*., 2009a; *Williamson et al*., 1996]. Given that glacially-fed lakes are often located at high elevations and/or latitudes and exposed to high-surface UVR, glacial ablation may result in substantial doses of UVR penetrating into the water column. Thus, documented glacial recession and ablation in many regions around the world [*Casassa et al*., 2009; *Hirabayashi et al*., 2010] may be producing rapid changes in light attenuation and the spectral composition of the underwater light field in these lakes [*Williamson et al*., 2001]. On shorter time scales, extreme events such as avalanches or intense storms may mobilize glacial flour from the watershed and have the potential to dramatically and rapidly decrease the transparency of glacially-fed lakes (J. M. Fischer and M. H. Olson, unpublished data, 2012–2013). The longer-term effects of such events in regulating variability or trends on water clarity are currently unknown.

Increases in transparency can have behavioral and physiological effects on aquatic organisms [*Rose et al*., 2009a; *Laspoumaderes et al*., 2013]. For example, UVR plays a strong role in regulating the diel vertical migration of zooplankton and can inhibit the colonization of invasive freshwater fish [*Tucker et al*., 2010; *Rose et al*., 2012; *Williamson et al*., 2011]. Thus, changes in glacial coverage may have important implications for the structure and function of glacially-fed lake ecosystems, the vulnerability of these ecosystems to colonization by invasive species, and the services these ecosystems provide.

Lakes are sentinels of broader environmental changes, and variations in light attenuation may be a particularly sensitive indicator of environmental change [*Williamson et al*., 2009]. Results here provide new insights into the optical characteristics of glacial flour and the relative contributions of glacial flour, DOC, water, and phytoplankton to light attenuation in glacially-fed lakes by providing turbidity-specific diffuse attenuation coefficients and quantifying the proportion of the diffuse attenuation coefficient represented by glacial flour. These insights provide new tools to better understand and forecast the effects of environmental change on glacially-fed ecosystems.

Acknowledgments

K.C.R. and C.E.W. received support from the National Science Foundation (NSF) Division of Graduate Education (DGE) Integrative Graduate Education Research and Traineeship (IGERT) grant 0903560. K.C.R. also received support from the Smithsonian Institution as a Smithsonian Postdoctoral Fellow. J.M.F. and M.H.O. received funding from Franklin and Marshall College and the Andrew W. Mellon Foundation through its grant in support of faculty development within the Central Pennsylvania Consortium. We acknowledge support for the New Zealand component of the study through the Ministry of Business, Employment and Innovation (contract UOWX0505). We thank the Parks Canada Agency for their permission to conduct our research in the national mountain parks of Canada (YNP-2008-1585). Field work on South American lakes (Negra and Lo Encañado) was supported by the NASA Planetary Lake Lander project (grant 10-ASTEP10-0011) and the SETI Institute. We thank Megan Rose, Jeremy Mack, Lucia Acosta, and Erin Overholt for assistance with field work and lab analyses. There are no supporting data for this manuscript.

References

Arar, E. J., and G. B. Collins (1997), Method 445.0: In vitro determination of chlorophyll a and pheophytin a in marine and freshwater algae by fluorescence, Cincinnati.

Binding, C. E., J. H. Jerome, R. P. Bukata, and W. G. Booty (2008), Spectral absorption properties of dissolved and particulate matter in Lake Erie, *Remote Sens. Environ.*, *112*(4), 1702–1711, doi:10.1016/j.rse.2007.08.017.

Bricaud, A., M. Babin, A. Morel, and H. Claustre (1995), Variability in the chlorophyll-specific absorption coefficients of natural phytoplankton: Analysis and parameterization, *J. Geophys. Res.*, *C7*(13), 321–332.

Casassa, G., P. López, B. Pouyaud, and F. Escobar (2009), Detection of changes in glacial run-off in alpine basins: Examples from North America, the Alps, central Asia and the Andes, *Hydrol. Process.*, *23*, 31–41, doi:10.1002/hyp.7194.

Chanudet, V., and M. Filella (2009), Size and composition of inorganic colloids in a peri-alpine, glacial flour-rich lake, *Geochim. Cosmochim. Acta*, *72*(5), 1466–1479, doi:10.1016/j.gca.2008.01.002.

Downing, B. D., B. A. Pellerin, B. A. Bergamaschi, J. F. Saraceno, and T. E. C. Kraus (2012), Seeing the light: The effects of particles, dissolved materials, and temperature on in situ measurements of DOM fluorescence in rivers and streams, *Limnol. Oceanogr. Methods*, *10*, 767–775, doi:10.4319/lom.2012.10.767.

Gallegos, C. L., D. L. Correll, and J. W. Pierce (1990), Modeling spectral diffuse attenuation, absorption, and scattering coefficients in a turbid estuary, *Limnol. Oceanogr.*, *35*(7), 1486–1502.

Gallegos, C. L., R. J. Davies-Colley, and M. Gall (2008), Optical closure in lakes with contrasting extremes of reflectance, *Limonol. Oceanogr.*, *53*(5), 2021–2034.

Hamilton, D., I. Hawes, and R. Davies-Colley (2004), Physical and chemical characteristics of lake water, in *Freshwaters of New Zealand*, edited by J. Harding et al., pp. 21.1–21.19, New Zealand Hydrological Society and New Zealand Limnological Society, Christchurch.

Hamilton, D. P., C. G. McBride, D. Özkundakci, M. Schallenberg, P. Verburg, M. de Winton, D. Kelly, C. Hendy, and W. Ye (2013), Effects of climate change on New Zealand lakes, in *Climate Change and Inland Waters: Impacts and Mitigation for Ecosystems and Societies*, edited by C. R. Goldman, M. Kumagai, and R. D. Robarts, pp. 337–366, John Wiley, West Sussex.

Hirabayashi, Y., P. Döll, and S. Kanae (2010), Global-scale modeling of glacier mass balances for water resources assessments: Glacier mass changes between 1948 and 2006, *J. Hydrol.*, *390*(3–4), 245–256, doi:10.1016/j.jhydrol.2010.07.001.

Hylander, S., et al. (2011), Climate-induced input of turbid glacial meltwater affects vertical distribution and community composition of phyto- and zooplankton, *J. Plankton Res.*, *33*(8), 1239–1248, doi:10.1093/plankt/fbr025.

Immerzeel, W. W., L. P. H. van Beek, and M. F. P. Bierkens (2010), Climate change will affect the Asian water towers, *Science*, *328*(328), 1382–1385, doi:10.1126/science.1183188.

Jonasz, M., and G. R. Fournier (2007), *Light Scattering by Particles in Water: Theoretical and Experimental Foundations*, Elsevier, New York.

Kirk, J. T. O. (1994), *Light and Photosynthesis in Aquatic Ecosystems*, 2nd ed., Cambridge Univ. Press, Cambridge.

Laspoumaderes, C., B. Modenutti, M. S. Souza, M. Bastidas Navarro, F. Cuassolo, and E. Balseiro (2013), Glacier melting and stoichiometric implications for lake community structure: Zooplankton species distributions across a natural light gradient, *Global Change Biol.*, *19*(1), 316–326, doi:10.1111/gcb.12040.

Laurion, I., M. Ventura, J. Catalan, R. Psenner, R. Sommaruga, N. Sep, and I. Latirion (2000), Attenuation of ultraviolet radiation in mountain lakes: Factors controlling the among- and within-lake variability, *Limnol. Oceanogr.*, *45*(6), 1274–1288.

Lee, Z.-P., K.-P. Du, and R. Arnone (2005), A model for the diffuse attenuation coefficient of downwelling irradiance, *J. Geophys. Res.*, *110*, C02016, doi:10.1029/2004JC002275.

Markager, S., and W. F. Vincent (2000), Spectral light attenuation and the absorption of UV and blue light in natural waters, *Limnol. Oceanogr.*, *45*(3), 642–650.
Modenutti, B., G. Pérez, E. Balseiro, and C. Queimaliños (2000), The relationship between light attenuation, chlorophyll a and total suspended solids in a Southern Andes glacial lake, *Verhandlungen des Int. Verein Limnol.*, *27*, 1–4.
Morris, D. P., H. Zagarese, C. E. Williamson, E. G. Balseiro, B. R. Hargreaves, B. Modenutti, R. Moeller, and C. Queimalinos (1995), The attenuation of solar UV radiation in lakes and the role of dissolved organic carbon, *Limnol. Oceanogr.*, *40*(8), 1381–1391.
Mudry, D. R., and R. S. Anderson (1975), Yoho National Park: Aquatic resources inventory.
Pechar, L. (1987), Use of an acetone:methanol mixture for the extraction and spectrophotometric determination of chlorophyll-a in phytoplankton, *Arch. Fur Hydrobiol.*, *78*(1), 99–117.
Pope, R. M., and E. S. Fry (1997), Absorption spectrum (380–700 nm) of pure water. 2. Integrating cavity measurements, *Appl. Opt.*, *36*(033), 8710–8723.
Quickenden, T. I., and J. A. Irvin (1980), The ultraviolet absorption spectrum of liquid water, *J. Chem. Phys.*, *72*(8), 4416, doi:10.1063/1.439733.
Rae, R., C. Howard-Williams, I. Hawes, A. M. Schwarz, and W. F. Vincent (2001), Penetration of solar ultraviolet radiation into New Zealand lakes: Influence of dissolved organic carbon and catchment vegetation, *Limnology*, *2*(2), 79–89, doi:10.1007/s102010170003.
Read, J. S., and K. C. Rose (2013), Physical responses of small temperate lakes to variation in dissolved organic carbon concentrations, *Limnol. Oceanogr.*, *58*(3), 921–931, doi:10.4319/lo.2013.58.3.0921.
Rose, K. C., C. E. Williamson, J. E. Saros, R. Sommaruga, and J. M. Fischer (2009a), Differences in UV transparency and thermal structure between alpine and subalpine lakes: Implications for organisms, *Photochem. Photobiol. Sci.*, *8*, 1244–56, doi:10.1039/b905616e.
Rose, K. C., C. E. Williamson, S. G. Schladow, M. Winder, and J. T. Oris (2009b), Patterns of spatial and temporal variability of UV transparency in Lake Tahoe, California-Nevada, *J. Geophys. Res.*, *114*, G00D03, doi:10.1029/2008JG000816.
Rose, K. C., C. E. Williamson, J. M. Fischer, S. J. Connelly, M. Olson, A. J. Tucker, and D. A. Noe (2012), The role of ultraviolet radiation and fish in regulating the vertical distribution of Daphnia, *Limnol. Oceanogr.*, *57*(6), 1867–1876, doi:10.4319/lo.2012.57.6.1867.
Roy, J. W., and M. Hayashi (2009), Multiple, distinct groundwater flow systems of a single moraine-talus feature in an alpine watershed, *J. Hydrol.*, *373*(1–2), 139–150, doi:10.1016/j.jhydrol.2009.04.018.
Saros, J. E., S. J. Interlandi, S. Doyle, T. J. Michel, and C. E. Williamson (2005), Are the deep chlorophyll maxima in alpine lakes primarily induced by nutrient availability, not UV avoidance?, *Arctic. Antarct. Alp. Res.*, *37*(4), 557–563, doi:10.1657/1523-0430(2005)037[0557:ATDCMI]2.0.CO;2.
Saros, J. E., K. C. Rose, D. W. Clow, V. C. Stephens, A. B. Nurse, H. A. Arnett, J. R. Stone, C. E. Williamson, and A. P. Wolfe (2010), Melting alpine glaciers enrich high-elevation lakes with reactive nitrogen., *Environ. Sci. Technol.*, *44*(13), 4891–4896, doi:10.1021/es100147j.
Slemmons, K. E. H., and J. E. Saros (2012), Implications of nitrogen-rich glacial meltwater for phytoplankton diversity and productivity in alpine lakes, *Limnol. Oceanogr.*, *57*(6), 1651–1663, doi:10.4319/lo.2012.57.6.1651.
Slemmons, K. E. H., J. E. Saros, and K. Simon (2013), The influence of glacial meltwater on alpine aquatic ecosystems: A review, *Environ. Sci. Process Impacts*, *15*(10), 1794–806, doi:10.1039/c3em00243h.
Sommaruga, R., R. Psenner, E. Schafferer, K. A. Koinig, and S. Sommaruga-Wögrath (1999), Dissolved organic carbon concentration and phytoplankton biomass in high-mountain lakes of the Austrian Alps: Potential effect of climatic warming on UV underwater attenuation, *Arct. Antarct. Alp. Res.*, *31*(3), 247–253.
Stambler, N., C. Lovengreen, and M. M. Tilzer (1997), The underwater light field in the Bellingshausen and Amundsen Seas (Antarctica), *Hydrobiologia*, *344*, 41–56.
Stubbins, A., et al. (2012), Anthropogenic aerosols as a source of ancient dissolved organic matter in glaciers, *Nat. Geosci.*, *5*(3), 198–201, doi:10.1038/ngeo1403.
Tucker, A. J., C. E. Williamson, K. C. Rose, J. T. Oris, S. J. Connelly, M. H. Olson, and D. L. Mitchell (2010), Ultraviolet radiation affects invasibility of lake ecosystems by warm-water fish, *Ecology*, *91*(3), 882–90.
Vant, W. N., and R. J. Davies-Colley (1984), Factors affecting clarity of New Zealand lakes, *N.Z. J. Mar. Freshwater Res.*, *18*(3), 367–377.
Vinebrooke, R. D., P. L. Thompson, W. Hobbs, B. H. Luckman, M. D. Graham, and A. P. Wolfe (2010), Glacially mediated impacts of climate warming on alpine lakes of the Canadian Rocky Mountains, *Verhandlungen des Int. Verein Limnol.*, *30*(9), 1449–1452.
Watras, C. J., P. C. Hanson, T. L. Stacy, K. M. Morrison, J. Mather, Y.-H. Hu, and P. Milewski (2011), A temperature compensation method for CDOM fluorescence sensors in freshwater, *Limnol. Oceanogr. Methods*, *9*, 296–301, doi:10.4319/lom.2011.9.296.
Williamson, C. E., and K. C. Rose (2009), Ultraviolet insights: Attempting to resolve enigmatic patterns in pelagic freshwaters—The historical context and a view to the future, *Int. Rev. Hydrobiol.*, *94*(2), 129–142, doi:10.1002/iroh.200811099.
Williamson, C. E., and K. C. Rose (2010), When UV meets fresh water, *Science*, *329*, 637–639, doi:10.1126/science.1191192.
Williamson, C. E., R. S. Stemberger, D. P. Morris, T. M. Frost, and S. G. Paulsen (1996), Ultraviolet radiation in North American lakes: Attenuation estimates from DOC measurements and implications for plankton communities, *Limonol. Oceanogr.*, *41*(5), 1024–1034, doi:10.4319/lo.1996.41.5.1024.
Williamson, C. E., P. J. Neale, G. Grad, H. J. De Lange, and R. H. Bruce (2001), Beneficial and detrimental effects of UV on aquatic organisms: Implications of spectral variation, *Ecol. Appl.*, *11*(6), 1843–1857.
Williamson, C. E., J. E. Saros, and D. W. Schindler (2009), Sentinels of change, *Science*, *323*(5916), 887–888.
Williamson, C. E., J. M. Fischer, S. M. Bollens, E. P. Overholt, and J. K. Breckenridge (2011), Towards a more comprehensive theory of zooplankton diel vertical migration: Integrating ultraviolet radiation and water transparency into the biotic paradigm, *Limnol. Oceanogr.*, *56*(5), 1603–1623, doi:10.4319/lo.2011.56.5.1603.